

## Shell-Mode Response of Buried Pipelines to Large Fault Movements

Shiro Takada\*, Jian-Wen Liang\*\* and Tengyan Li\*\*\*

\*Fellow of JSCE, Dr. of Eng., Professor, Dept. of Civil Eng., Kobe University, Rokkodai, Nada, Kobe 657, Japan

\*\*Member of ASCE, Associate Professor, Dept. of Civil Eng., Tianjin University, Tianjin 300072, China

\*\*\*Member of JSCE, Assistant Professor, Dept. of Civil Eng., Kobe University, Rokkodai, Nada, Kobe 657, Japan

This paper deals with shell-mode response of pipelines to large fault movements by geometrically nonlinear finite element algorithm, in which the pipeline is discretized into 4-node thin shell elements with elasto-plastic material characteristics, and soil is modeled by nonlinear springs. The calculated results are in a good agreement with the experimental data, and the parametric studies have been carried out on soil stiffness, fault type, fault slip angle, and ratio of diameter to thickness of pipe, etc. The results have shown that it is necessary to estimate the shell-mode response for seismic design of a pipeline across a fault, especially in the case of a reverse fault.

Key Words: shell-mode response, buried pipeline, large fault movement

### 1. Introduction

Many post-earthquake investigations indicated that pipelines suffered from serious damages due to large fault movements, and performance of pipelines across faults during an earthquake have been paid great attentions<sup>1)-6)</sup>. But, until now, all the research were focused on beam-mode response of pipelines, which may be due to the simplicity for analysis. In reality, pipelines behave more like a shell when crossing a fault, especially for large-diameter pipelines. Therefore, it is necessary to have a try to analyze this problem by a shell model.

Usually, fault movement can be divided into three types<sup>7)</sup>: strike, normal and reverse faults which were shown in Figure 1. Post-earthquake investigations also showed that different performances of pipelines would occur for different types of fault movements, and pipelines were more susceptible to reverse fault movement<sup>8)</sup>. However, most of present researches were only involved in normal faults, which may be because of the difficulty in analyzing buckling of pipelines due to reverse fault movement using beam models<sup>1)-6)</sup>.

This paper deals with shell-mode response of pipelines to large normal and reverse fault movements by geometrically nonlinear finite element algorithm, in which the pipeline is discretized into 4-node thin shell elements, with elasto-plastic material characteristics, and soil is modeled by nonlinear springs. The calculated results are in a good agreement with the experimental data, and the parametric studies have been carried out on soil stiffness, fault type, fault slip angle, and ratio of diameter to thickness of pipe, etc. The results can be a reference for seismic design of pipelines across a fault.

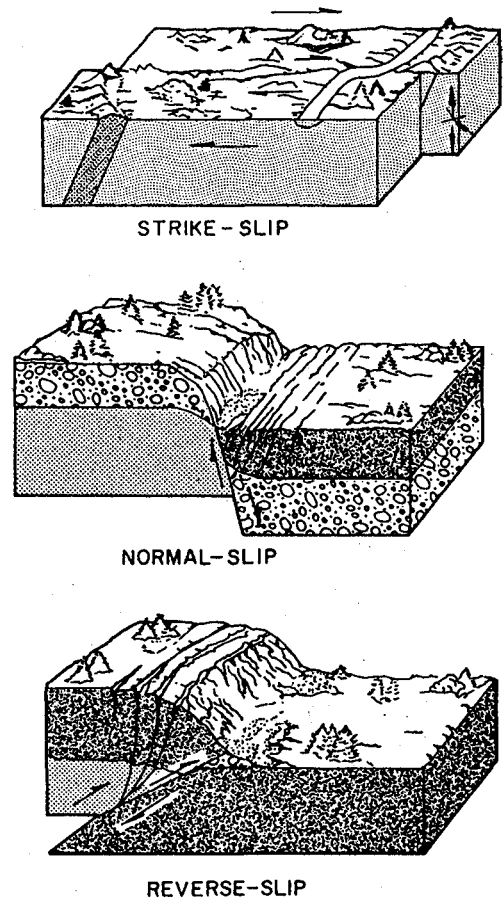
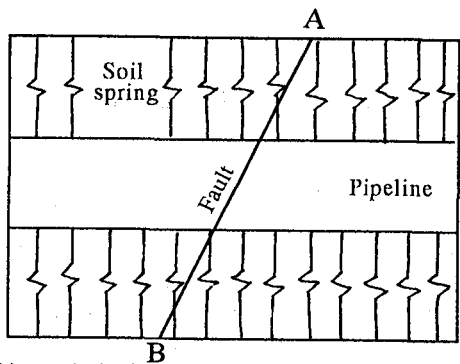
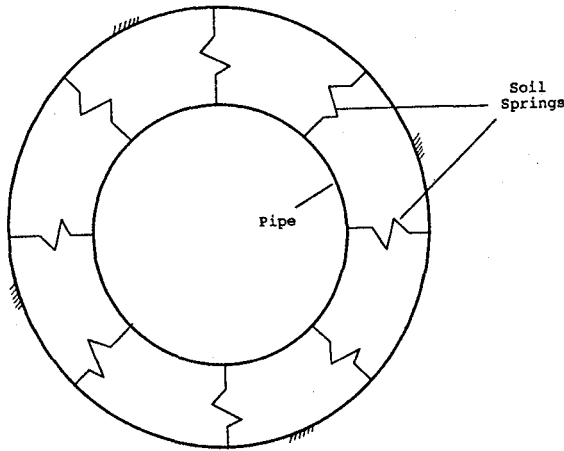


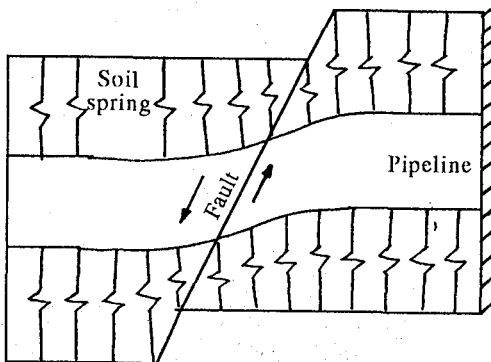
Figure 1. Types of fault movements<sup>7)</sup>



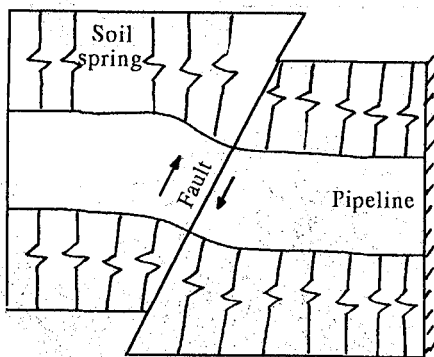
(a) Analytical model for longitudinal section



(b) Analytical model for cross section



(c) Model for normal fault movement



(d) Model for reverse fault movement

Figure 2. The Model

## 2. Model

To simplify the problem, a simple pipeline-spring system model (Figures 2 (a) and (b)) is put forward, in which, the pipeline is discretized by 4-node shell elements, and soil by springs, and the one ends of the springs are connected with the nodes of the shell elements, and the another ends are given forced displacements to simulate the fault movements (Figures 2 (c) and (d)).

The 4-node doubly curved shell elements are used to discretize the pipeline (Figure 3), which can be used for geometrically nonlinear analysis and elasto-plastic material characteristics. The diameter and thickness of the calculational model are 0.762m and 0.019m.

The stress-strain relation of the material of steel pipelines is shown in Figure 4, in which, the elastic modulus is  $2.1E+11$ Pa, and yield stress  $3.66E+8$ Pa, and hardening stress  $5.5E+8$ Pa at a strain of 5%.

The soil is discretized by spring elements in three directions: one axial and two transverse direction, whose force-displacement relations of the soil are shown in Figure 5. The elastic coefficient of soil is taken as  $9.E+6$ Pa or variable, and slippage takes when relative displacement reaches at  $1.667E-3$ m. We assume that for radial springs, the stiffness of soil in the compression direction will not vary, but in tension direction, the stiffness is set 1/10 of that in compression direction, and the separation will take place when relative displacement reaches at  $1.667E-3$ m; for axial and hoop springs, same force-displacement relations are considered.

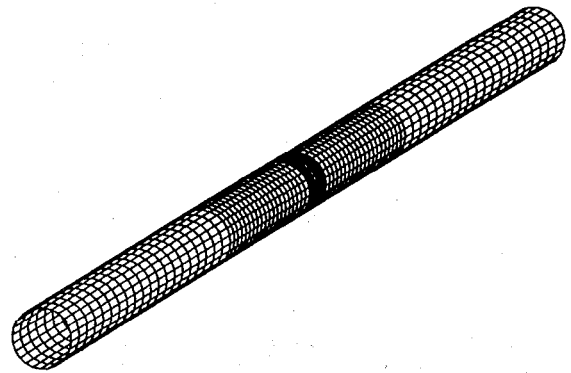


Figure 3. Discretization of pipeline

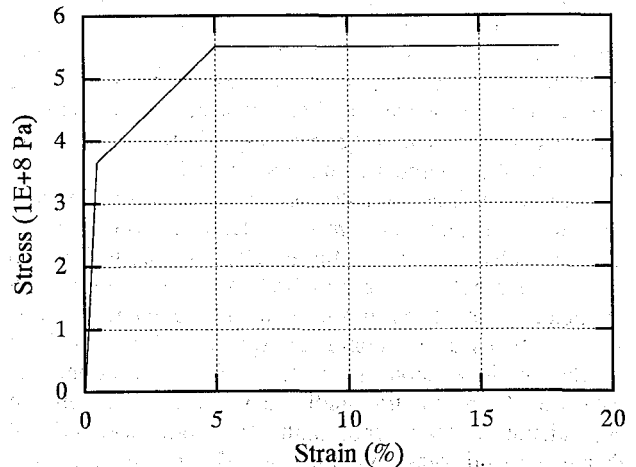
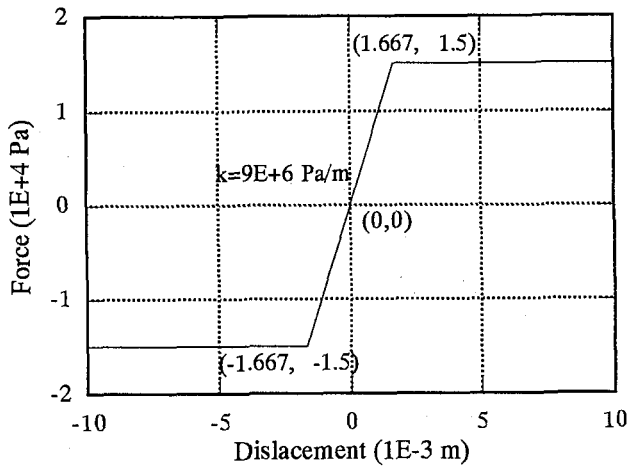
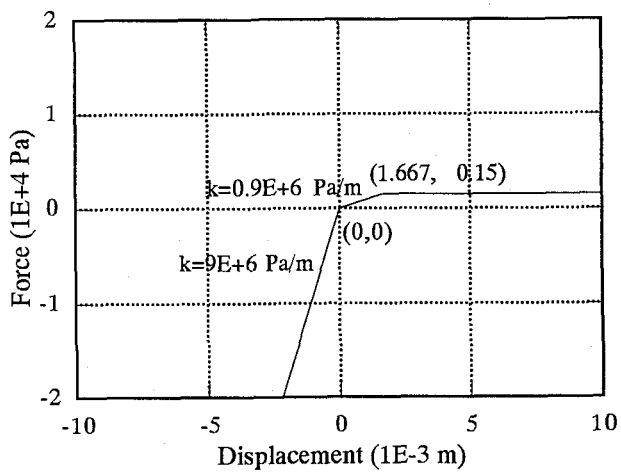


Figure 4. Stress-strain relation of pipeline material



(a) Axial and hoop direction



(b) Radial direction

Figure 5. Force-displacement relations of soil spring

### 3. Parametric studies

#### 3.1 Determination of model length of pipelines

At first, let's determine the acceptable model length of pipelines. Usually, this length should be very long. Kennedy et al<sup>8)</sup> pointed that it should be at least 1200 feet (366 meter), which is easily applied for beam-mode analysis, but for shell-mode calculation, this length is too long to be calculated for the limitation of memory and time of computers; on the other hand, it is not necessary to conduct such calculations because we only care for the behavior of a pipeline near the fault.

Due to the reasons above, we have a try for different model length  $L=20D$ ,  $30D$  and  $40D$  ( $D$  is pipe diameter) for normal fault 45 degree case, and Figure 6 and Figure 7 give the results for the two highest strain values of two elements (No.1266 and 258 on two sides of B) with the increment of fault displacement. From the two figures we can find that when  $L=30D$  and  $40D$ , the strain values tend to the same. So, we choose  $L=30D$  as the acceptable model length of pipelines for the save of memory and time of computers.

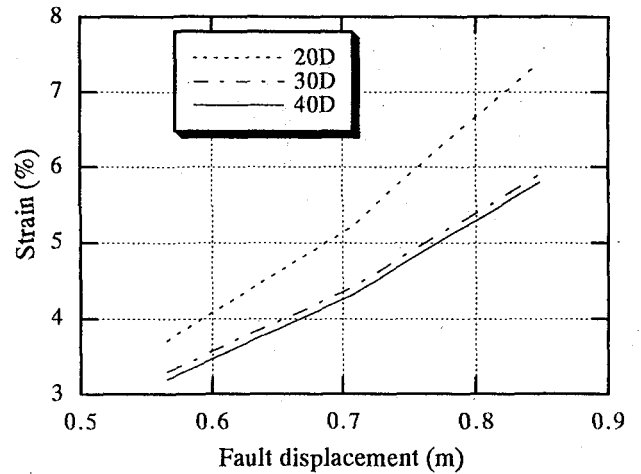


Figure 6. The relation between pipe strain and fault displacement (element No.1266)

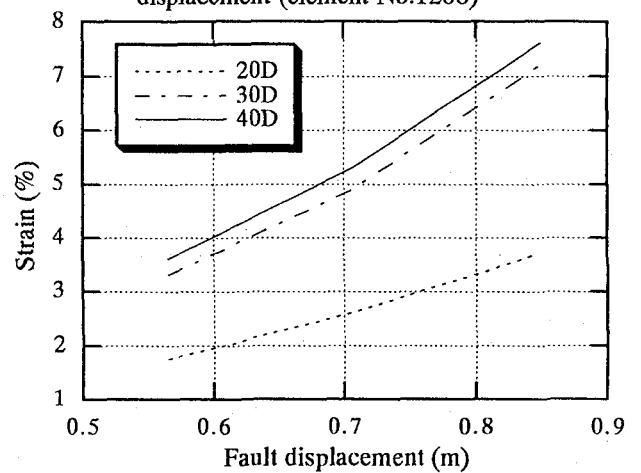


Figure 7. The relation between pipe strain and fault displacement (element No.258)

#### 3.2 Comparison with experimental data

In order to verify the calculated results, we make a comparison with the experimental data<sup>9-10)</sup> for buried pipes subjected to large ground settlement. The experiment used<sup>10)</sup> sinking-soil-box to give large ground deformation.

The calculated highest tension strains and experimental data are at same position, both at the top of pipes in the fixed side, about 50cm to the boundary. Figure 8 is the comparison between the calculated results and experimental data. From the comparison, we can find that before the yielding of pipeline material (elastic modulus  $2.1E+6Pa$ , yielding stress  $2.4E+8Pa$ )<sup>9)</sup> at strain 0.114% the calculated results are in good agreement with the experimental data, however, after the yielding, there is a big difference, which may be due to that there exists soil failures in actual experimental case and that we can only assume a constant stiffness after slippage between soil and pipeline for calculation case. On the whole, the calculation results can be verified by the experimental data.

#### 3.3 Typical normal fault with 45 degree case

Now, we show some responses of pipelines with 45

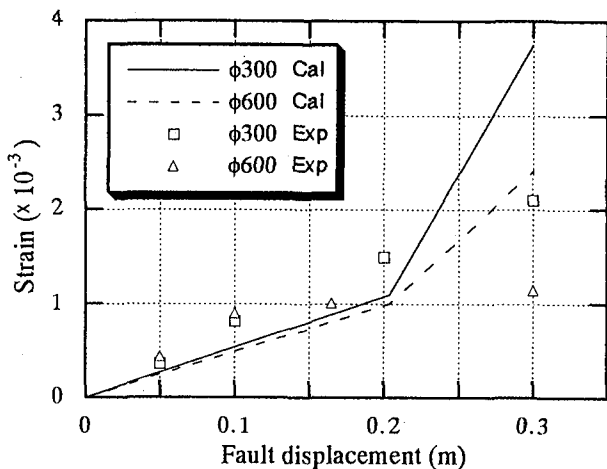


Figure 8. Comparison between calculated and experimental results

degree typical normal fault movement with displacement 1.0m. Figures 9 to 10 are the axial and hoop strain contours, and Figures 11 to 12 are the principal strain contours. We can find that the distribution of axial strain is almost the same as that of maximum principal strain, and the distribution of hoop strain is almost same as the minimum principal strains, and the axial strain is much higher than the hoop strain, which indicates that in normal fault case axial tension strain governs the response of the pipeline, and we also can find that higher axial strain distributes along the fault plane.

The variation of maximum axial strain (composed by elastic and plastic strain) with fault displacement is shown in Figure 13, from which we can know that the plastic strain predominates the total strain, which takes more than 97%, and the plastic strain increases more and more quickly as the increment of fault displacement. This could illustrate the importance of ductility of steel pipelines when crossing a fault.

Figure 14 shows the distribution of axial strain at the top of the pipeline with fault displacement 0.5m and 1.0m. We can find from the figure that maximum axial strain appears at fault plane, and much higher than that at other positions along the pipeline, and the axial strain decreases very quickly, and due to the compression, the minimum axial strain appears at left symmetric position.

### 3.4 Typical reverse fault with 45 degree case

Next, we give some responses of pipelines for 45 degree typical reverse fault movement to displacement 0.5m. Figures 15 to 16 are the axial and hoop strain contours, and Figures 17 to 18 are the principal strain contours. From these figures we can find that the distribution of axial strain is almost same as that of minimum principal strain, and the distribution of hoop strains is almost same as the maximum principal strain, and the axial strain is higher than the hoop strain, which indicates that in reverse fault case axial compression strain controls the response of the pipeline.

Another important phenomenon is local buckling when the fault displacement is 0.325m (axial strain about 5%), and we can find that the strain concentrations are

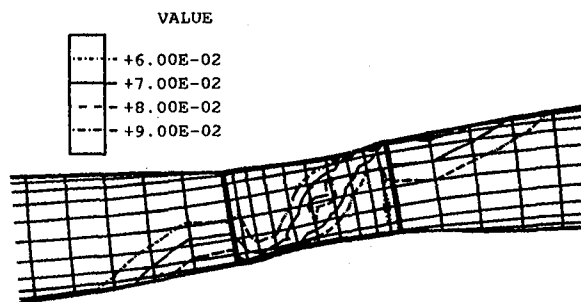


Figure 9. Axial strain contours

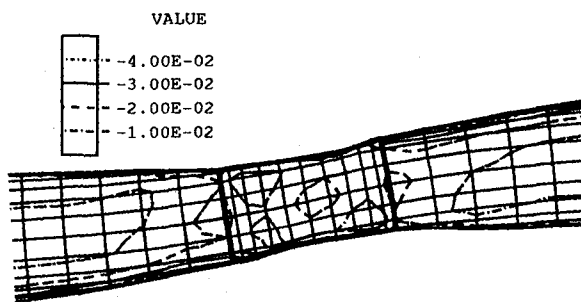


Figure 10. Hoop strain contours

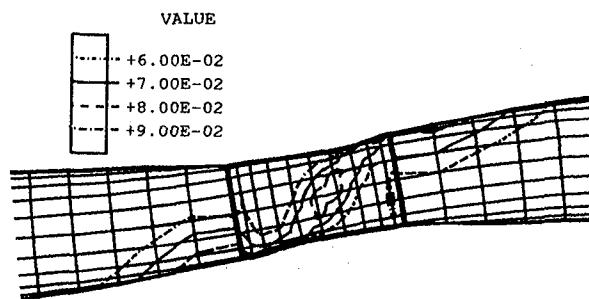


Figure 11. Maximum principal strain contours

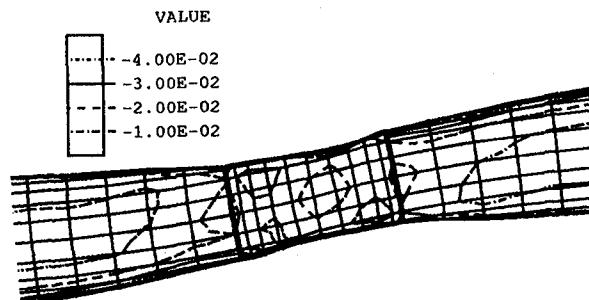


Figure 12. Minimum principal strain contours

very high at the buckling positions. After the buckling, the strains redistribute, and the redistribution of strain at buckling of top of the pipe is shown in Figure 19, from which we can find that the strains in element 558 and 510 have little change, but the strain in element 534 increases very quickly from -5% to -18.76%. The buckling appears at strain about 5%, which is right the hardening strain

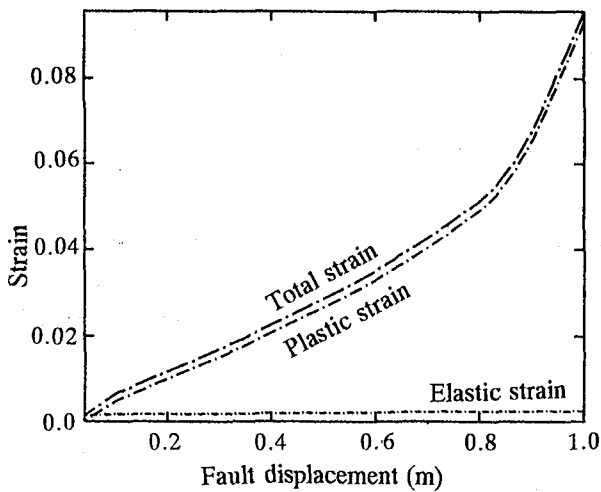


Figure 13. Variation of total, elastic and plastic strain with fault movement (element No.1266)

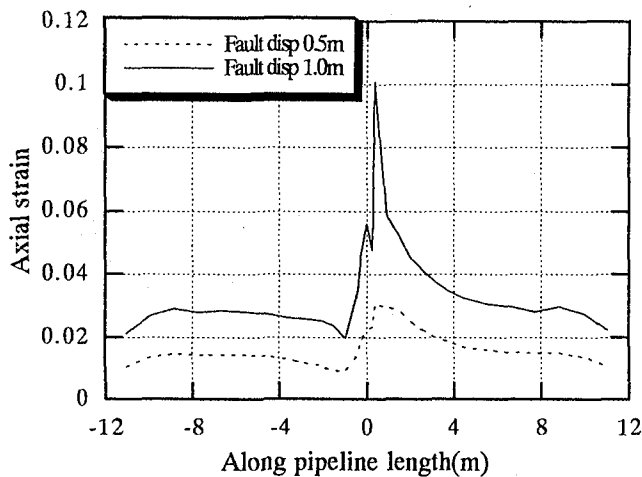


Figure 14. Variation of strain distribution along pipeline at fault displacement 0.5m and 1.0m

of steel, so we can know that the amplitude of hardening strain controls the collapse of the shell-mode failure of a pipeline, and the pipeline can resist very high local strain (e.g., 5%) till to its collapse. Figure 20 shows the distribution of axial strain at the top of the pipeline with fault displacement 0.3m and 0.5m. From this figure, we can find that the distributions of strain with fault displacement 0.3m (before buckling) and 0.5m (after buckling) are almost the same except the strains at buckling position, and the strain at buckling position is increased by 3-4 times.

### 3.5 Allowable strain criterion

Allowable fault displacement is a comprehensive parameter measuring the ability of a pipeline to resist fault movements, and can be defined as the fault displacement corresponding to the allowable maximum strain for pipeline material. Hereafter, we will use this parameter for parametric studies.

Kennedy et al<sup>7)</sup> said in their paper that API 5LX-Grade 52 and 60 steel pipe can be reliable withstand average tensile strain over significant length in excess of 5%

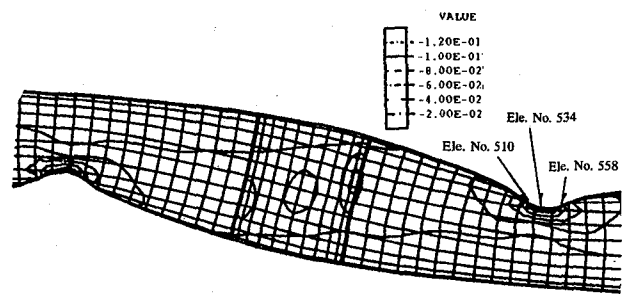


Figure 15. Axial strain contours

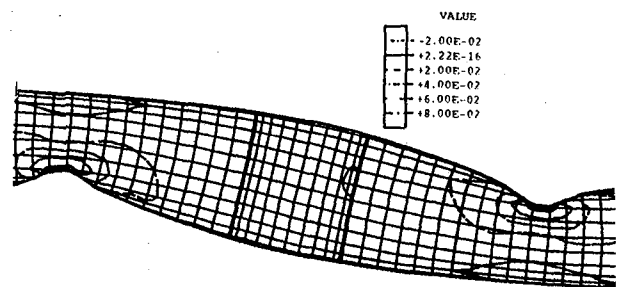


Figure 16. Hoop strain contours

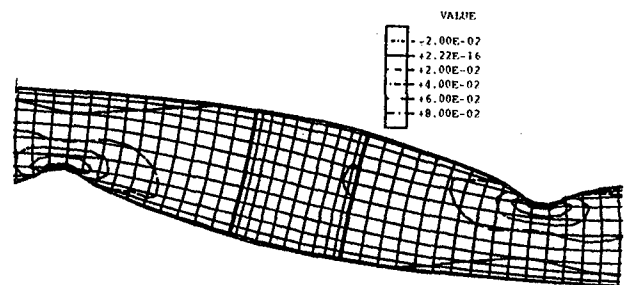


Figure 17. Maximum principal strain contours

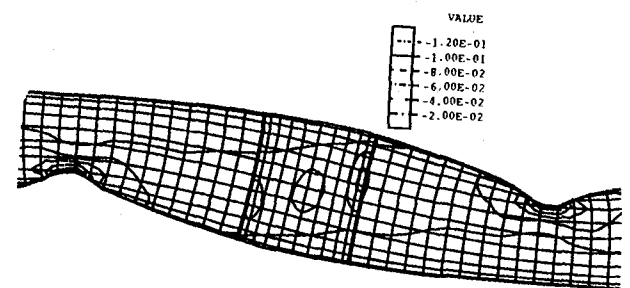


Figure 18. Minimum principal strain contours

without rupture, and local strain concentration could be much higher in excess of 15%, but the pipe is not as ductile by large compressive strains, about 0.4-0.6% with a diameter to thickness ratio of 100. For the buckling only in pure axial compression. The Earthquake Resistant Design Guideline of Gas Pipes<sup>11)</sup> of Japan Gas Association gave some experimental data about strain 2-3% for usual ratio of diameter to thickness.

In this paper, we use hardening strain (e.g., 5%) both for the allowable maximum tension and compression strain based on the stress-strain relation (Figure 5) and the

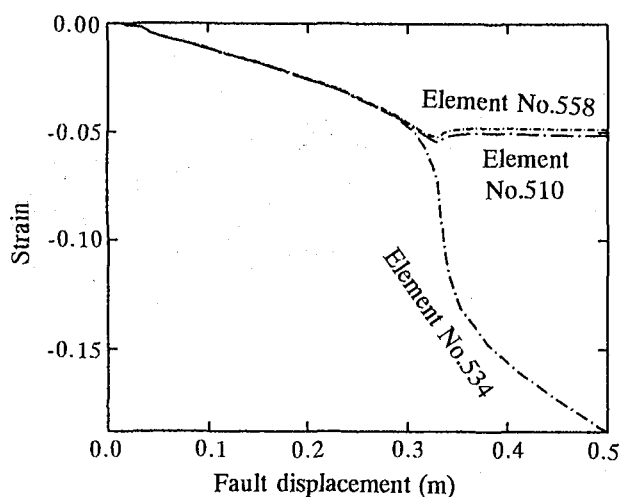


Figure 19. Variation of strains at buckling position

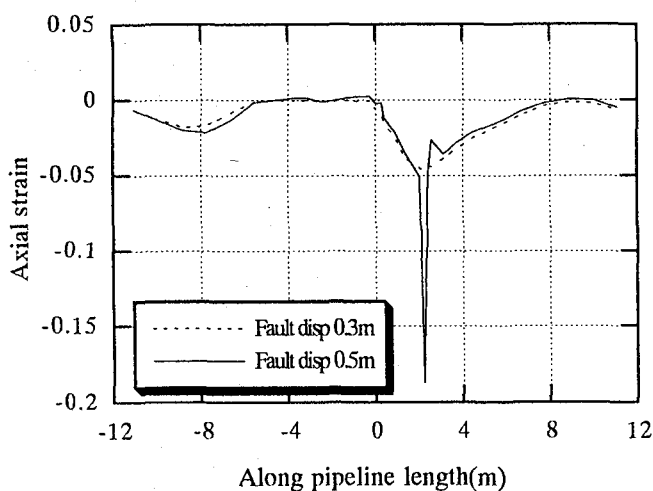


Figure 20. Variation of strain distribution along pipeline with fault displacement 0.3m (before buckling) and 0.5m (after buckling)

strain variation curves in normal fault case (Figure 13) and reverse fault case (Figure 19), since this value is easily used to explain the damage of a pipeline in this research. However, it should be noted that different material should have different hardening strain value, and the value 5% will not affect our conclusions.

### 3.6 Effect of soil stiffness

Soil stiffness is one of the most important parameters affecting the response of a pipeline. Figure 21 shows the allowable fault displacement curves at different soil stiffness for normal fault 30, 45, 60 and 90 degree case. From this figure we can find that as the increase of soil stiffness, the allowable fault displacements decrease, and among 30, 45 and 60 degree cases, the allowable fault displacement in 30 degree case has the highest value. For fault displacement 1.0m, the displacements in axial and transverse direction are 0.866m and 0.5m for 30 degree case, 0.707m and 0.707m for 45 degree case, and 0.5m and 0.866m for 60 degree case. So, the effect of soil stiffness on a pipeline is greater in transverse direction than in axial direction in normal case. It should be noted

that 90 degree is a special case for normal fault, and also has the same conclusion, but the allowable fault displacement decreases most quickly.

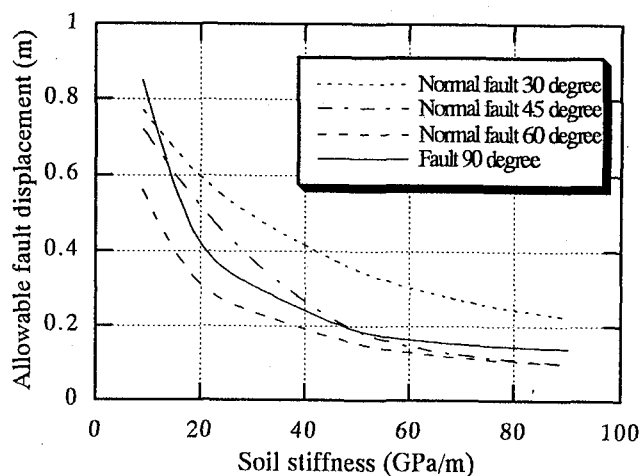


Figure 21 Effect of soil stiffness on normal fault

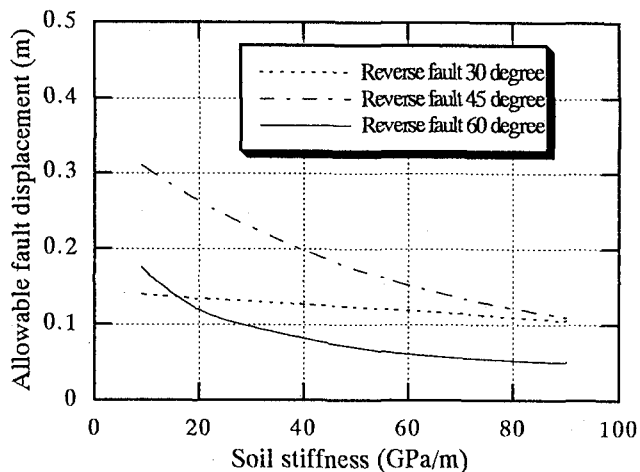
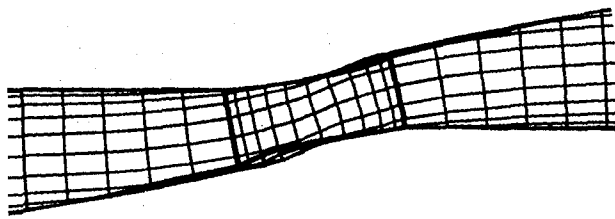


Figure 22 Effect of soil stiffness on reverse fault

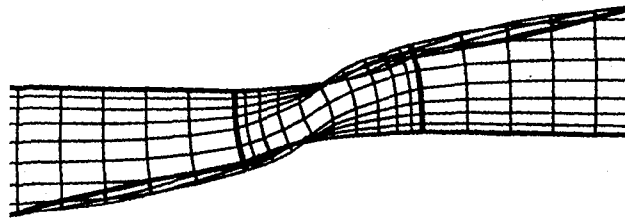
For reverse fault, there are the same conclusions as the normal fault case that as the soil stiffness increases, the allowable fault displacements decrease (Figure 22). But, in the case of 30 degree, the allowable fault displacement is small and varies only a little as the increase of soil stiffness. From Figure 22, we also can know that the allowable fault displacement is highest in the case 45 degree other than the 30 and 60 degree case, which may be studied further.

The deformed shapes at different soil stiffness for normal and reverse fault cases are shown in Figures 23 and 24, and (a) for 18GPa/m, (b) for 45GPa/m and (c) for 90GPa/m. From these figures, we can understand the effect of soil stiffness on the response of the pipeline more easily.

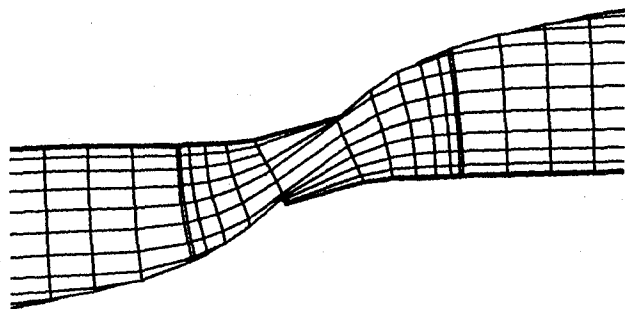
Figure 25 compares the effect of soil stiffness on normal and reverse fault movement, from which we can know that a pipeline is more susceptible to reverse fault than normal fault, but as the increase of soil stiffness, normal and reverse fault have the same effect on pipelines.



(a) Soil stiffness (18 GPa/m)

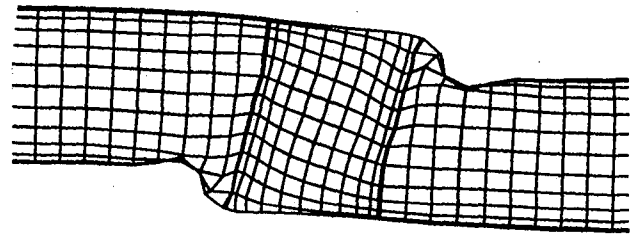


(b) Soil stiffness (45 GPa/m)

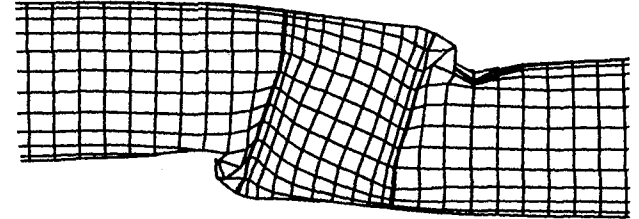


(c) Soil stiffness (90 GPa/m)

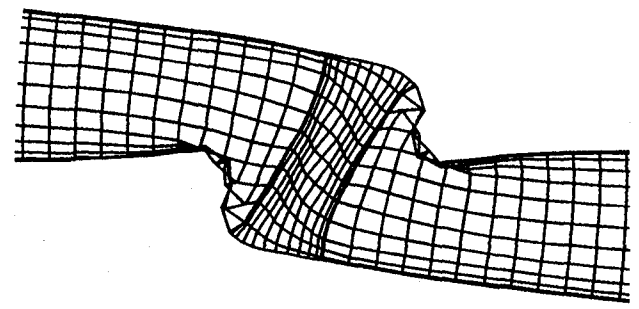
Figure 23. Deformed shape for different soil stiffness (normal fault case)



(a) Soil stiffness (18 GPa/m)



(b) Soil stiffness (45 GPa/m)



(c) Soil stiffness (90 GPa/m)

Figure 24. Deformed shape for different soil stiffness (reverse fault case)

### 3.7 Effect of fault slip angle

From the analyses above, we have some knowledge that fault slip angle is another very important parameter affecting pipeline response. Figures 26 to 28 show the relation between the allowable fault displacement and the fault slip angle for different soil stiffness 9GPa/m, 18GPa/m and 45GPa/m. From these figures we can find that in normal fault case small slip angle will be benefit for pipelines, and 60 degree is the most unfavourable one; but in reverse fault case, 45 degree is the most favourable and 60 degree still the most serious one; and as the increasement of soil stiffness, the fault effect on a pipeline will tend to the same for different fault slip angles both in normal and reverse fault cases.

### 3.8 Effect of diameter-to-thickness ratio

Figure 29 shows the relation between allowable fault diaplacement and the dismeter-to-thickness ratio for three cases: normal fault with 45 degree, reverse fault with 45 degree and strike fault with 90 degree. From the figure we can find that as the increasement of the ratio the allowable fault displacement decreases, and this tells us that thicker pipelines will increase the ability to resist fault movements, which may be an effective countermeasures for seismic design.

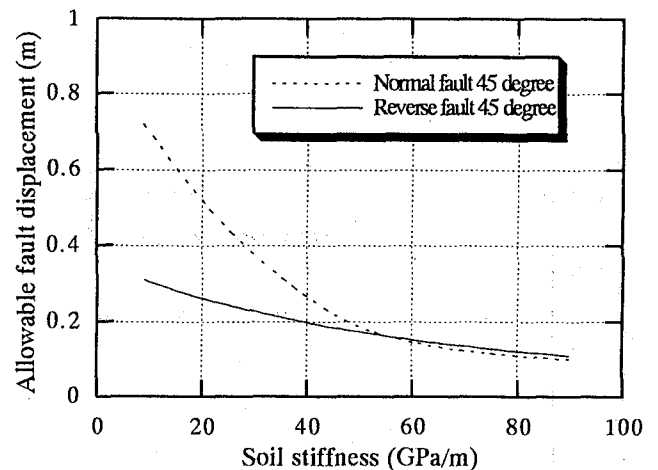


Figure 25. Effect of soil stiffness on normal and reverse fault

### 3.9 Comparison with beam model

In order to verify the shell model further, we make some comparison between shell model and beam models<sup>1,3,6</sup>.

The model<sup>1)</sup> by Newmark and Hall is the earliest one on this subject, which advised the shallow burial for pipelines acrossing faults, so the pipelines could displace

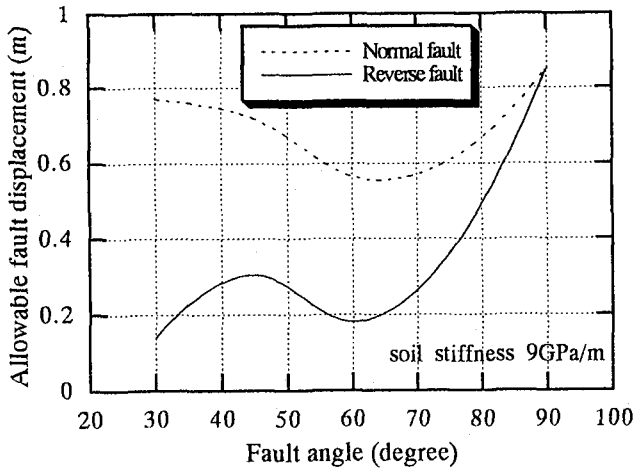


Figure 26. Effect of fault type and angle (soil stiffness 9GPa/m)

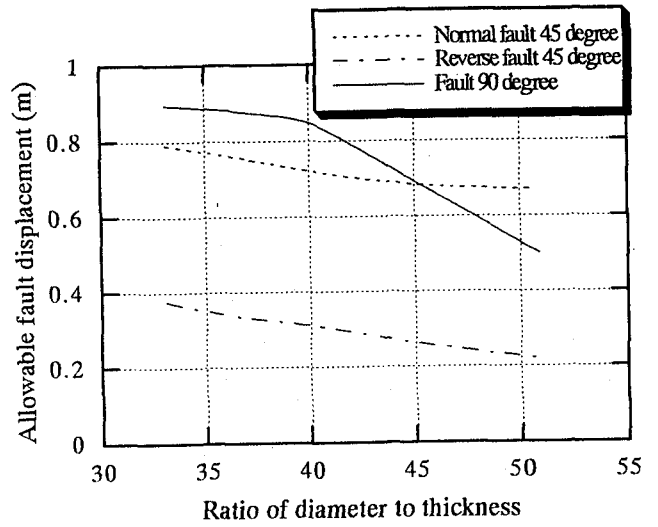


Figure 29. Effect of ratio of diameter to thickness

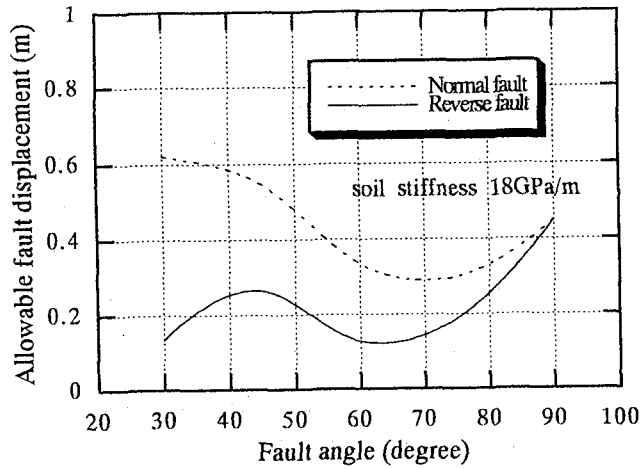


Figure 27. Effect of fault type and angle (soil stiffness 18GPa/m)

Table 1. Comparison with Newmark's model

Model	Allowable fault displacement (m)			
	Fault angle	30 degree	45 degree	60 degree
Newmark <sup>3)</sup>		2.64	3.23	4.57
Present Paper		0.77	0.72	0.56

Table 2 Comparison with Ford's model (normal fault movement)

Model	Normal fault (displacement 1.0m)			
	Fault angle	30 degree	45 degree	60 degree
Ford <sup>3)</sup>		3.82%	3.16%	2.28%
Present Paper		7.10%	9.59%	12.20%

Table 3 Comparison with Ford's model (reverse fault movement)

Model	Reverse fault (displacement 0.5m)			
	Fault angle	30 degree	45 degree	60 degree
Ford <sup>3)</sup>		-1.88%	-1.53%	-1.07%
Present Paper		-20.90%	-18.76%	-17.31%

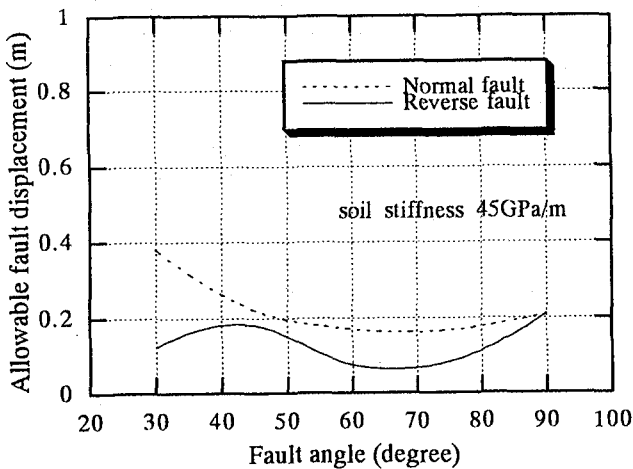


Figure 28. Effect of fault type and angle (soil stiffness 45GPa/m)

out of soil, and based on this viewpoint they used the average strain for the design, in which the hardening strain of pipeline material was used for the average strain.



However, the model is difficult to be applied for deep buried depth, since usually pipelines could not displace out of soil. Here, the method is used for comparison of allowable fault displacement. Table 1 gives the allowable fault displacement for normal fault movement. It should be noted that the model by Newmark and Hall can only be used for normal faults, and has no relation with soil stiffness due to pipelines out of soil. The results of present model in Table 1 is for the soil stiffness 9Gpa/m. We can find that there is a great difference, which tells us shallow burial is a very effective countermeasure for the seismic design of pipelines acrossing faults.

Tables 2 and 3 show the comparison of maximum axial strain with beam model given by Ford<sup>3)</sup>, and from which we can find there is great difference between the shell model and the beam model, too. The main reason may be due to that the Ford model can only consider elastic behavior of pipelines, which may result in an inadequate estimation.

The present authors have also compared the shell model with the beam model by Takada<sup>6)</sup>, and some conclusions have been obtained<sup>6)</sup> that in the case of normal faults the distribution of strain is in a very good agreement between the shell model and the beam model, but in the case of reverse faults, there is a great difference, the reason of which may be that it is difficult to deal with the buckling by the beam model, so in the case of reverse fault, it is necessary to conduct shell-mode analysis.

### 3.10 3-D fault movements

Usually, fault movements are in three directions along fault plane, e.g., the combination of a normal fault or a reverse fault movement with a strike fault movement. Figures 30 to 31 show the deformed shape of the pipeline near the fault whose displacements are 1.0m (0.577m in three right crossing directions respectively) for the normal fault case and 0.5m (0.289m in three right crossing directions respectively) for the reverse fault case. From the figures we can find that the response of the pipeline is more complicated than that only in two-direction cases. Due to the complicated response, more studies on 3-D fault movement case are needed further.

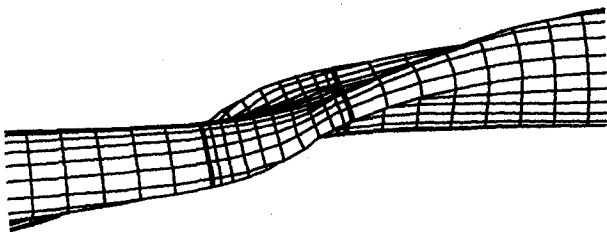


Figure 30. Deformed shape for 3-D normal fault

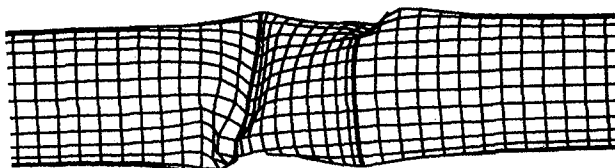


Figure 31. Deformed shape for 3-D reverse fault

## 4. Conclusions

From the parametric studies, following conclusions can be obtained:

- 1) The proposed model can estimate the shell-mode response of pipelines due to large fault movements
- 2) It is necessary to conduct shell-mode calculation for seismic design of pipelines across faults, especially for reverse fault movement, since the beam models could not deal with local buckling which governs the behavior of a pipeline due to a reverse fault movement.
- 3) Pipelines are more susceptible to reverse fault movement than normal fault movement due to local buckling, however the allowable strain could be up to the hardening strain of steel materials.
- 4) Axial strain governs the performance of pipelines to large fault movements, even in the case of 90 degree. The maximum strain appears in fault plane for normal fault case, but for a reverse fault, because of the local buckling the maximum strain will be at buckling positions.
- 5) The plastic strain predominates the total strains, and the plastic part can take more than 97%, which has shown the importance of the ductility of pipelines, so it is not enough only to calculate the elastic response of pipelines, which might lead to inadequate results.
- 6) Soil stiffness has very important effect on response of pipelines, and as the increasement of soil stiffness, the allowable fault displacement decreases. For a reverse fault movement, the buckling position will gradually move to the fault plane as the increasement of soil stiffness.
- 7) Fault slip angle is another important parameter affecting on the performance of pipelines, and in normal fault case small angle will be benefit for pipelines, and 60 degree is the most unfavourable case, but in reverse fault case, 45 degree is the most favourable and 60 degree is the most serious.
- 8) As the increasement of the ratio of diameter to thickness the allowable fault displacement decreases, so thicker pipelines will increase the ability to resist fault movements, which may be an effective countermeasures for seismic design.

## Acknowledgement

This research was carried out when the second author was visiting Kobe university as a postdoctoral research fellow on leaving from Tianjin University of China.

## References

- 1) Newmark, N.M. and Hall, W.J.: Pipeline design to resist large fault displacements, Proceedings of US National Conference on Earthquake Engineering, EERI, Oakland, pp.416-425, 1975.
- 2) Kennedy, R.P., Chow, A.W. and Williamson, R.A.: Fault movement effect on buried oil pipeline, Journal of Transportation Engineering, ASCE, Vol.103, pp.617-633, 1977.
- 3) Ford, D.B.: Joint design for pipelines subject to large ground deformations, PVP-Vol.77, ASME, pp.160-165, 1983.

4) Sato, H., Katsuki, S. and Ishikawa, N.: Elastic-plastic analysis of plane buried pipelines under forced ground deformation, Proceedings of JSCE, No.350, pp.217-226, 1984.(in Japanese).

5) Wang, L.R.L. and Yeh, Y.H.: A refined seismic analysis and design of buried pipelines for fault movement, Earthquake Engineering and Structural Dynamics, Vol.13, pp.75-96, 1985.

6) Takada, S., Li, T. and Liang, J.W.: Earthquake resistance analysis of pipelines to fault movements, Proceedings of 24th JSCE Symposium on Earthquake Engineering, Kobe, pp.969-972, 1997(in Japanese).

7) Taylor, C.L. and Cluff, L.S., Fault displacement and ground deformation associated with surface faulting, Proceedings of ASCE TCLEE Specialty Conference on Lifeline Earthquake Engineering, Los Angeles, pp.338-353, 1977.

8) Kennedy, R.P., Darrow, A.C. and Short, S.A.: General considerations for seismic design of oil pipeline systems, Proceedings of ASCE TCLEE Specialty Conference on Lifeline Earthquake Engineering, Los Angeles, pp.1-17, 1977.

9) Tanabe, K. and Takada, S.: Design formulae of buried pipes subjected to large ground settlement and its application, Proceedings of JSCE, No.374, pp.593-602, 1986(in Japanese).

10) Takada, S. and Yamabe, Y.: An experiment on a seismic behavior of buried pipelines subjected to large ground deformations using the sinking-soil-box, Proceedings of JSCE, No.323, pp.55-65, 1982(in Japanese).

11) Japan Gas Association: Earthquake Resistant Design Guideline of Gas Pipes, 1982(in Japanese).

(Received September 26, 1997)